Analysis of Red Blood Cell Motion through Cylindrical Micropores: Effects of Cell Properties

T. W. Secomb and R. Hsu
Department of Physiology, University of Arizona, Tucson, Arizona 85724 USA

ABSTRACT Filtration through micropores is frequently used to assess red blood cell deformability, but the dependence of pore transit time on cell properties is not well understood. A theoretical model is used to simulate red cell motion through cylindrical micropores with diameters of 3.6, 5, and 6.3 μm, and 11-μm length, at driving pressures of 100–1000 dyn/cm^2. Cells are assumed to have axial symmetry and to conserve surface area during deformation. Effects of membrane shear viscosity and elasticity are included, but bending resistance is neglected. A time-dependent lubrication equation describing the motion of the suspending fluid is solved, together with the equations for membrane equilibrium, using a finite difference method. Predicted transit times are consistent with previous experimental observations. Time taken for cells to enter pores represents more than one-half of the transit time. Predicted transit time increases with increasing membrane viscosity and with increasing cell volume. It is relatively insensitive to changes in internal viscosity and to changes in membrane elasticity except in the narrowest pores at low driving pressures. Elevating suspending medium viscosity does not increase sensitivity of transit time to membrane properties. Thus filterability of red cells is sensitively dependent on their resistance to transient deformations, which may be a key determinant of resistance to blood flow in the microcirculation.

INTRODUCTION

Red blood cells passing through microvessels must undergo large deformations. Therefore, the deformability of red cells is a key aspect of blood flow in the microcirculation. Several different experimental approaches have been developed to assess red cell deformability. In some techniques, the transit times of individual red cells across a membrane containing cylindrical micropores are measured optically or electrically (Kiesewetter et al., 1981; Frank and Hochmuth, 1987, 1988; Koutsouris et al., 1988; Fisher et al., 1992). Pore diameters in the range of 3 to 7 μm are used. In filtration tests, flow rates of red cell suspensions through membranes containing micropores are determined (Gregersen et al., 1967; Reinhard and Chien, 1985; Bucherer et al., 1988; Nash, 1990). The increase, caused by red cells, in the time required to filter a given volume is linearly related to the transit time of individual cells (Koutsouris et al., 1983).

Use of micropore transit to assess red cell deformability has the advantage that the pore diameters can be chosen to correspond with the diameters of the smallest microvessels. A further advantage is that red cells undergo transient deformations as they enter pores, and that the ability of red cells to undergo transient deformations may be an important aspect of their ability to circulate. However, one disadvantage is that the dependence of red cell transit time on the mechanical properties of red cells is not well understood. The complexity of the deformations undergone by red cells makes it difficult to deduce values of specific mechanical parameters from such measurements. In contrast, experiments based on observation of individual red cells aspirated into micropipettes, in combination with theoretical analyses (Evans and Skalak, 1980) permit the quantitative determination of membrane mechanical characteristics. Such information can be used to predict the motion and deformation of red cells in other geometries (Secomb, 1991).

The goal of this study was to analyze the motion of red cells through narrow cylindrical pores, using a theoretical model. Most of the key mechanical properties of the red cell were incorporated in the model, and the effects of changing these properties on cell transit time were predicted. The model predictions provide a basis for interpreting differences in transit time measurements in terms of the mechanical properties of red cells.

Few detailed theoretical studies have been made of red cell motion in cylindrical micropores. The motion of a red cell from a relatively large tube into a narrower cylindrical pore was analyzed by Skalak and Özkaya (1987). A numerical method based on boundary integral equations has been used by Drochon et al. (1994). Recently, Secomb and Hsu (1996) described a method for analyzing the motion of red cells through microvessels with irregular cross-sections, which will be used in the present study.

METHODS

Assumptions of the model

When a red blood cell passes through a cylindrical micropore in a membrane, it undergoes a complex, time-dependent, three-dimensional deformation, which depends on the geometry of the pore, the mechanical properties of the cell, and the flow of the suspending fluid. To allow analysis of this motion, several simplifications must be made, as outlined below and discussed in more detail by Secomb and Hsu (1996).

First, the geometries of both the cell and the pore are assumed to be axisymmetric. Red cells take on nonaxisymmetric shapes in pores (Rein-

Received for publication 3 November 1995 and in final form 2 May 1996.
Address reprint requests to Dr. Timothy W. Secomb, Department of Physiology, University of Arizona, Tucson, AZ 85724. Tel.: 520-626-4513; Fax: 520-620-1463; E-mail: secomb@ccit.arizona.edu.

0006-3495/96/08/1095/07 $2.00

hart et al., 1991), but the compression of the cell to a narrow cylindrical shape within the pore, which is an essential part of the deformation, can be represented by an axisymmetric model. Hsu and Secomb (1989) showed that nonaxisymmetry of red cell shape has little effect on the resistance to red cell motion in narrow uniform tubes. However, it should be noted that an axisymmetric model may not be adequate for predicting the changes in electrical resistance across a pore caused by red cell passage, because in reality red cells are typically folded over as they enter the pore, with a cleft or groove on one side that may provide the main pathway for electrical current.

Second, lubrication theory is used to analyze the flow of suspending fluid in the gap between the cell and the wall. This theory is based on the assumption that the gap is narrow compared with the other dimensions, and that the Reynolds number is very low. The validity of lubrication theory in problems of this type has been discussed by Halpern and Secomb (1991).

Third, a simplified representation of red cell mechanics is used. The viscoelastic behavior of the membrane in shear deformations is represented by a Kelvin solid model (Evans and Hochmuth, 1976). The membrane is assumed to deform without change in surface area. The interior of the cell is considered to be an incompressible fluid. Initially, internal viscosity is neglected; its effects are discussed below. The bending resistance of the membrane is neglected and shape of the trailing edge of the cell, whose curvature is controlled by bending resistance, is represented by a sharp cusp, according to the method developed by Secomb and Gross (1983). The axial component of membrane tension must vanish at this point.

Formulation of the model

Cylindrical polar coordinates (r,θ,z) are defined traveling with the cell, with origin at the front of the cell and z increasing toward the rear (Fig. 1a). A material coordinate σ is defined as the arc length measured along the cell from the origin in an axisymmetric reference shape. The radial position of a material element in the reference shape is denoted $r_0(\sigma)$. The position of material point σ at time t is given by $(r(\sigma,t), z(\sigma,t))$. Other variables are $s(\sigma,t)$, arc length measured along the cell from the origin; $\theta(\sigma,t)$, angle between the normal to the membrane and the axis; and $a(\sigma,t)$, pore radius.

With these assumptions, the extensions (stretch ratios) of the membrane in the axial and circumferential directions are $\lambda_s = \partial s/\partial\sigma$ and $\lambda_\phi = r/r_0$. Because the membrane deforms without change in area, $\lambda_s\lambda_\phi = 1$. According to the Kelvin solid model, the axial and circumferential components of membrane tension are (Evans and Skalak, 1980):

$$t_s = t_0 - t_d \quad \text{and} \quad t_\phi = t_0 + t_d$$

where

$$t_d = (2\mu_m/\lambda_\phi)\,(\partial\lambda_\phi/\partial t) + \kappa\,(\lambda_\phi^2 - \lambda_\phi^{-2})$$

and t_0 is the isotropic part of the membrane tension.

The equations for equilibrium of normal and tangential forces on the membrane are:

$$p_0 - p = \partial\theta/\partial s\, t_s + r^{-1}\sin\theta\, t_\phi$$

and

$$r^{-1}\partial(rt_s)/\partial s = r^{-1}\cos\theta\, t_\phi - \tau_c$$

where p_0 is the constant pressure in the cell interior, p is the pressure in the gap, and τ_c is the fluid shear stress on the membrane. These equations may be rearranged to give

$$p_0 - p = (r/r_0)\,\partial\theta/\partial\sigma\, t_s + r^{-1}\sin\theta\,(t_s + 2\,t_d) \quad (1)$$

and

$$(r/r_0)\,\partial t_s/\partial\sigma = 2r^{-1}\cos\theta\, t_d - \tau_c \quad (2)$$

An axisymmetric formulation of lubrication theory is used (Fitz-Gerald, 1969). The hydrostatic pressure within the gap is assumed to be constant across the gap, but to vary along it, and the transverse component of velocity is neglected. The axial velocity profile in the gap is calculated in terms of the pressure gradient, and the flow rate and shear stress on the membrane are deduced. The spatial derivative of the flow rate is related to the time derivative of the gap width by conservation of volume. This approach leads to a time-dependent lubrication equation:

$$-\frac{1}{16\mu}\frac{\partial}{\partial\sigma}\left[(a^2-r^2)\left(a^2+r^2-\frac{a^2-r^2}{\ln(a/r)}\right)\frac{\partial p/\partial\sigma}{\partial z/\partial\sigma}\right] + \frac{1}{4}\frac{\partial^2 z}{\partial\sigma\,\partial t}\left(\frac{a^2-r^2}{\ln(a/r)} - 2r^2\right) + \frac{1}{4}\left(\frac{\partial z}{\partial t} - u_0\right)\frac{\partial}{\partial\sigma}\frac{a^2-r^2}{\ln(a/r)} - r\frac{\partial z}{\partial\sigma}\frac{\partial r}{\partial t} = 0 \quad (3)$$

and an expression for the fluid shear stress on the membrane:

$$\tau_c = \frac{1}{4}\frac{\partial p/\partial\sigma}{\partial z/\partial\sigma}\left(2r - \frac{a^2-r^2}{r\ln(a/r)}\right) - \frac{\mu}{r\ln(a/r)}\left(\frac{\partial z}{\partial t} - u_0\right)$$

In regions where both the wall and the cell membrane are inclined at a significant angle to the vessel axis, these equations are modified as described by Secomb and Hsu (1996).

Eqs. 1–3 are expressed in finite-difference form, with 70 to 90 nodal values of σ at a spacing $\Delta\sigma \simeq 0.1$ μm, and a time step Δt corresponding to cell movement of ~0.01 μm. The radius of curvature of the concave rear part of the cell and the position of the trailing edge are determined to give the correct cell volume and surface area. The driving pressure Δp across the pore is held constant, and the cell shape and position are computed as functions of position and of time. Poiseuille's law is used to estimate the pressure drop in the part of the pore not occupied by the red blood cell. The additional pressure drop in this region due to an adjacent cell is negligible (Secomb et al., 1986).

This procedure yields predictions of the cell's shape and position as functions of time. In addition, the resistance to flow in the pore (defined as the ratio of driving pressure to flow rate) and the rates of energy dissipation

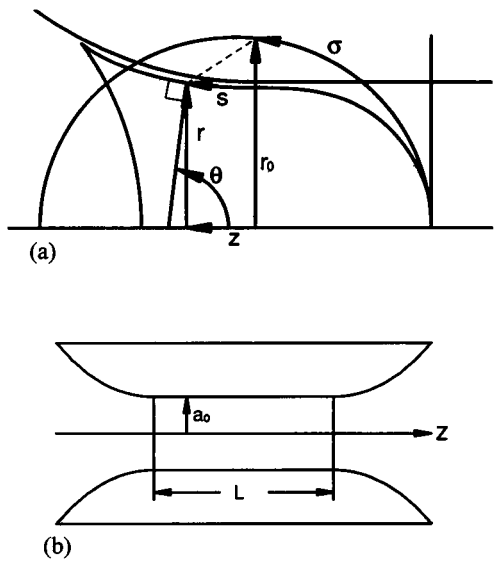

FIGURE 1 (*a*) Variables describing cell shape. Semicircle denotes reference shape. Dashed line links corresponding points in reference and deformed shapes. (*b*) Pore geometry.

in the cell membrane and in the surrounding fluid are computed as functions of time.

Pore geometries and parameter values

The lubrication approach used here requires that the pore have a smoothly defined profile, without sharp corners. Pore shapes used in the simulations are given by:

$$a = \begin{cases} a_0 + \alpha a_0(\cosh \lambda Z - 1) & \text{if } Z < 0 \\ a_0 & \text{if } 0 \le Z \le L \\ a_0 + \alpha a_0(\cosh \lambda (Z - L) - 1) & \text{if } Z > L \end{cases}$$

where L is the length of the cylindrical part of the pore, Z is axial distance measured from its entrance and a_0 is its radius (Fig. 1 *b*). Pores with diameters $2a_0$ = 3.6 μm, 5 μm and 6.3 μm, and length L = 11 μm are considered, corresponding to the observations of Frank and Hochmuth (1987, 1988). The parameters α and λ determine the shape of the entrance and exit regions. Assuming α = 1.8 and λ = 0.2 μm^{-1} results in constrictions with smooth but quite rapid transitions (Fig. 1 *b*) qualitatively similar to the pores in a nickel filter described by Nakamura et al. (1994), which have rounded edges. However, the more frequently used polycarbonate filters contain pores that are nearly cylindrical, with sharply defined edges at the entrance and exit. Possible effects of this difference for cell transit are discussed below.

The following standard parameter values are assumed for a normal human red blood cell: membrane shear viscosity, μ_m = 0.001 dyn·s/cm; and membrane elastic shear modulus, κ = 0.006 dyn/cm. Effects of membrane shear elasticity and viscosity on transit time are examined by considering the effect of doubling these parameters. The reference configuration for the membrane (in which $\lambda_s = \lambda_\phi = 1$) is chosen as a sphere with the same surface area (135 μm^2) (Secomb et al., 1986). Normal cell volume is set to 90 μm^3, and the effects of changes in volume are tested by using values ranging from 80 to 100 μm^3. Driving pressures in the range 100–1000 dyn/cm^2 are assumed. The reference suspending medium viscosity is assumed to be 0.01 dyn·s/cm^2. Higher viscosities are also used to examine the effects of suspending medium viscosity on transit time. An initially lens-like cell shape is chosen for convenience. Possible effects of initial cell shape on transit time are discussed below.

The transit time of a red cell through a pore is defined as the period during which the resistance to flow in the pore exceeds its baseline level (no red cell) by at least 20%. Because resistance typically rises rapidly when the cell enters the pore, the estimate of transit time is not sensitive to this choice of threshold. The entrance time of a red cell is defined as the part of the transit time during which the rate of energy dissipation in the membrane exceeds 5% of the total viscous dissipation in the cell and surrounding fluid (excluding fluid upstream or downstream of the cell). This represents the period during which most of the cell deformation occurs as it enters the pore, and ends when the cell is wholly within the cylindrical part of the pore.

RESULTS

Fig. 2 shows sequences of cell shapes computed at equally spaced time increments, for pores with diameters 3.6, 5, and 6.3 μm, at a driving pressure of 1000 dyn/cm^2. Cells underwent large, rapid deformations as they entered pores, and then traveled through the pores and exited them with little change in shape.

The resistance to cell motion in a 5-μm pore is shown both as a function of position and as a function of time in Fig. 3. It is expressed as relative resistance, normalized with respect to its value when no red cell is present (7.2×10^9 dyn·s/cm^5, in this case). At each instant, the product of the

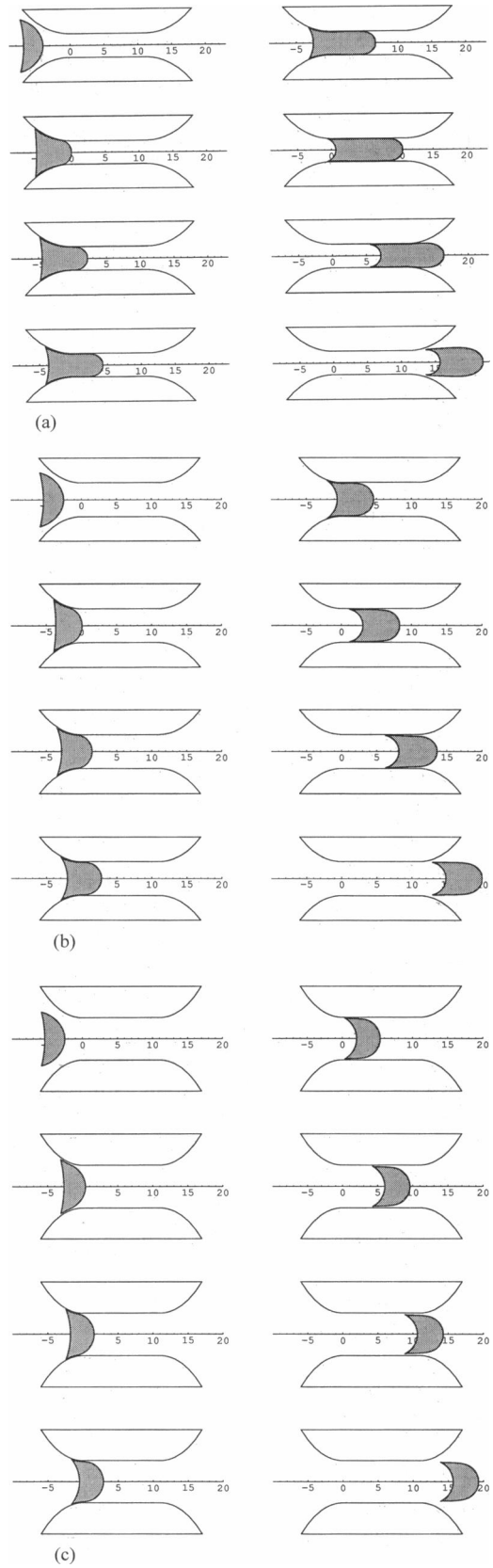

FIGURE 2 Sequences of computed cell shapes, at equal time increments (Δt), for driving pressure 1000 dyn/cm^2. Axis is scaled in μm. (*a*) Diameter = 3.6 μm, Δt = 8.3 ms. (*b*) Diameter = 5 μm, Δt = 2 ms. (*c*) Diameter = 6.3 μm, Δt = 0.7 ms.

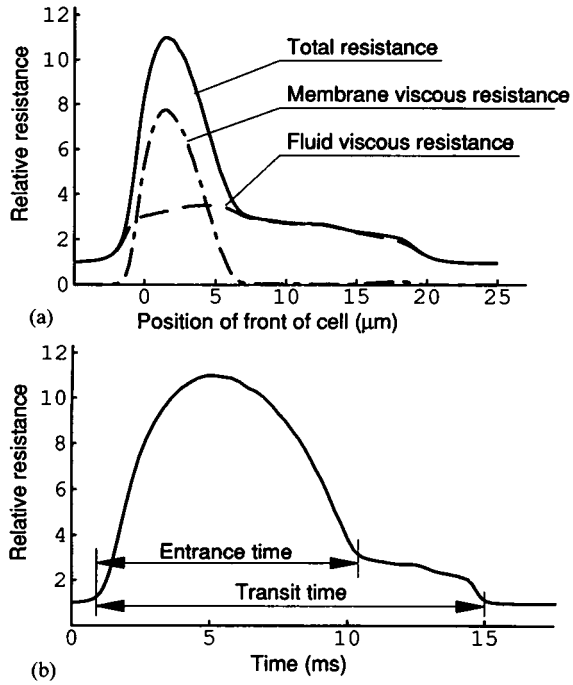

FIGURE 3 Resistance to cell motion in a pore with diameter of 5 μm, at a driving pressure of 1000 dyn/cm^2, relative to the resistance with no red cell present. (*a*) Plotted as a function of position. Contributions of viscous dissipation in the lubrication layer and in the membrane are indicated. (*b*) Plotted as a function of time.

driving pressure and the flow rate equals the total rate at which work is being done on the cell and suspending fluid. This has three components: viscous dissipation in the fluid, viscous dissipation in the membrane, and elastic energy storage in the membrane (Fig. 3 *a*). The elastic contribution was negligible in this case. During the entrance phase, most of the resistance was associated with viscous dissipation in the membrane. The relatively large resistance during this phase slowed the red cell, and the entrance time represented 67% of the total transit time (Fig. 3 *b*). Once the cell was within the pore, membrane deformation was slight and the resistance resulted from viscous drag in the lubrication layer.

In all cases considered, including variations in pore size, driving pressure, membrane properties, and suspending medium viscosity, the entrance time represented ~50% to 75% of the total transit time. This shows the importance of the red cell deformation during the entrance phase in determining the transit time.

Predicted transit times for normal cells are shown in Fig. 4 for a range of pore sizes and driving pressures. For a given driving pressure, transit time is a sensitive function of pore size. For example, transit times for 3.6-μm pores were 12–14 times greater than for 6.3-μm pores. As expected, transit time decreased with increasing driving pressure. At higher driving pressures, transit time varied almost in inverse proportion to pressure. This property may be used to predict transit times for driving pressures >1000 dyn/cm^2, based on the results presented here.

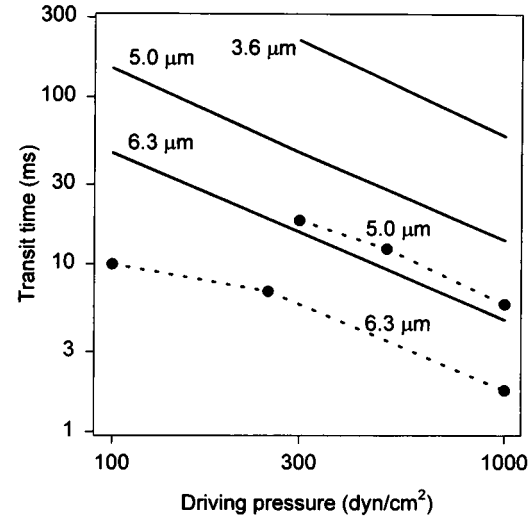

FIGURE 4 Transit times of normal cells in pores with diameters as indicated, as functions of driving pressure. Solid lines: present results. Dots: experimental results of Frank and Hochmuth (1987).

Fig. 4 also includes experimentally measured transit times for 5- and 6.3-μm pores. These times were deduced from the cell velocity data of Frank and Hochmuth (1987). The variation of transit time with pore size and driving pressure was very similar to the theoretical predictions. However, the measured times were consistently lower than the predicted times by a factor of two to four. Possible reasons for this difference are discussed below.

Transit time depends on cell volume. Throughout the ranges of pore diameters and driving pressures considered, an increase of cell volume from 90 μm^3 to 100 μm^3 resulted in a 3–5% increase of transit time, whereas a 10-μm^3 decrease in volume led to a 5–6% reduction in transit time.

Fig. 5 illustrates the effects of membrane shear viscosity

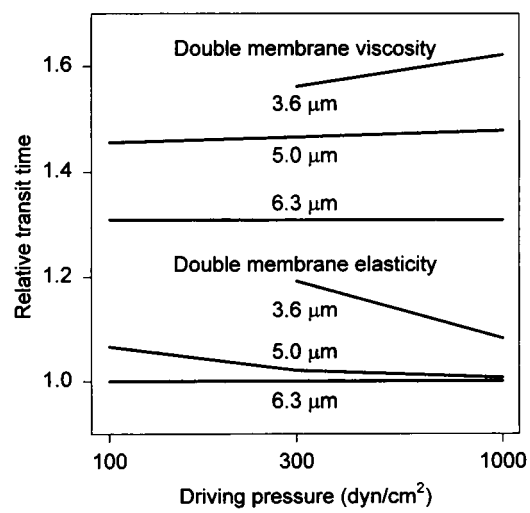

FIGURE 5 Effect of doubling membrane shear viscosity or elasticity on transit time, for pores with diameters as indicated, as a function of driving pressure. Transit time is expressed relative to transit time for normal cells.

and elasticity on transit time. Doubling membrane viscosity resulted in a 56–62% increase of cell transit time for a 3.6-μm pore, 46–48% for a 5-μm pore, and 31% for a 6.3-μm pore. These effects were only slightly dependent on the driving pressure used. In contrast, the effect of shear elasticity on transit time was strongly dependent on both the size of the pore and the driving pressure. Transit time in 6.3-μm pores was virtually unchanged by doubling shear elasticity over the range of pressures considered here. A slight increase was seen in 5-μm pores, particularly at low driving pressure (7% at 100 dyn/cm^2). In 3.6-μm pores, transit time showed a marked sensitivity to membrane shear elasticity as driving pressure decreased. For pressures >1000 dyn/cm^2, however, the model predicted that transit time was insensitive to shear elasticity, even in 3.6-μm pores.

As expected, transit time increased with increasing suspending medium viscosity (Fig. 6). The increase was less than linear with viscosity. For example, a fourfold increase in medium viscosity led to an increase in transit time by a factor ranging from 2 to 3 in each case. This reflects the contribution of membrane viscosity to the resistance to cell motion.

The sensitivity of transit time to membrane properties is shown in Fig. 7 as a function of suspending medium viscosity. As viscosity was increased, the increase in transit time resulting from increased membrane viscosity became less significant. This was to be expected, as increasing the suspending medium viscosity decreases the relative role of membrane viscosity in determining resistance to cell motion. In contrast, the effect of membrane elasticity on transit time was insensitive to changes in suspending medium viscosity, at a fixed driving pressure.

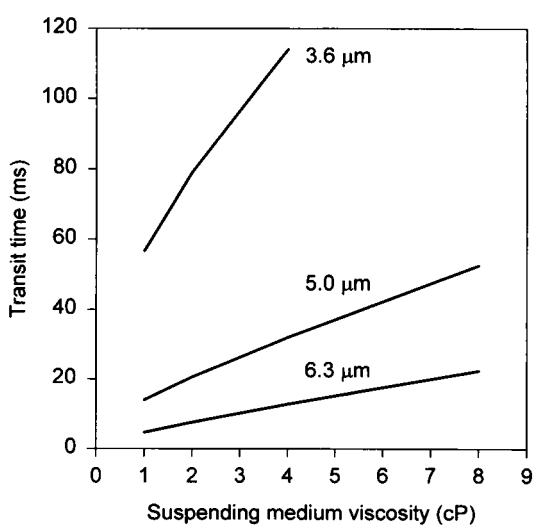

FIGURE 6 Effect of suspending medium viscosity on transit time of normal cells for pores with diameters as indicated at a driving pressure of 1000 dyn/cm^2.

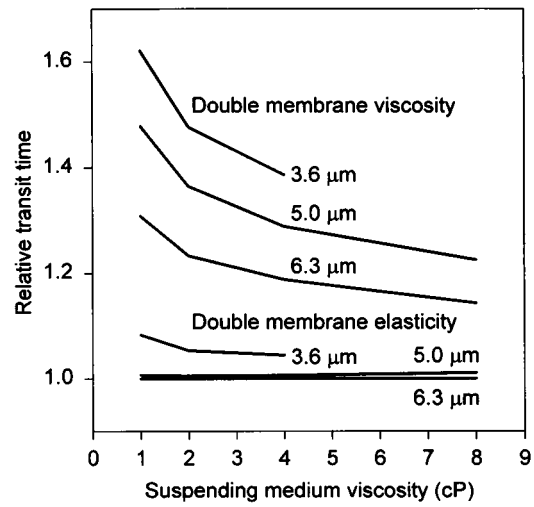

FIGURE 7 Effect of doubling membrane shear viscosity or elasticity on transit time for pores with diameters as indicated as a function of suspending medium viscosity, at a driving pressure of 1000 dyn/cm^2. Transit time is expressed relative to transit time for normal suspending medium viscosity.

DISCUSSION

Micropore filtration experiments are often used to examine the deformability of red blood cells. However, results of such experiments have been difficult to interpret in terms of specific mechanical properties of red blood cells, and their implications for blood flow in vivo have not been clear (Nash, 1990; Lipowsky et al., 1993). Theoretical models provide a method for predicting the dependence of micropore transit times on cell properties. Such predictions should provide a basis for more precise and quantitative interpretations of filtration data in terms of the mechanics of red cells and their ability to traverse the circulatory system. The theoretical model presented here differs from previous analyses of micropore filtration in that the equations of membrane equilibrium were formulated including the effects of membrane viscosity. As already shown, membrane viscosity strongly influenced micropore transit time.

Predicted transit times were consistently higher than the experimental values obtained by Frank and Hochmuth (1987). Comparisons with other experimental data (Kiesewetter et al., 1981; Koutsouris et al., 1988; Fisher et al., 1992) led to the same conclusion. However, the definition of transit time used in experiments is generally based on the period during which the electrical resistance pulse exceeds a threshold value, e.g., 55% of its peak value. This results in substantially shorter transit times than would be obtained with the definition used here. The present model did not predict the shape of the resistive pulse, so the extent of this difference cannot be estimated quantitatively.

Another possible explanation for the difference between predicted and observed transit times is the assumption of axisymmetric geometries in the model. This corresponds to a red cell approaching the pore face-on and deforming into a cup shape as it enters, and it implies a substantial degree

of membrane shear. A cell probably more typically approaches edge-on, and adapts to the pore partly by folding. This deformation may involve lower resistance to pore transit. The magnitude of this difference can be estimated by considering different (axisymmetric) initial shapes. The initial cell shape assumed above had a diameter of 8 μm. If a more highly curved initial shape, with a diameter of 7 μm and an unchanged volume, is assumed instead, the transit time for a 6.3-μm pore is reduced by ~20%. For smaller pores, the ultimate deformation is greater, and the effect of initial shape is correspondingly less. Note also that membrane elastic properties influence initial cell shape, and the possible consequent effects on transit time are not taken into account here.

The experimental data were derived from pores with relatively sharp edges, but the model assumes pores with flared entrance and exit regions. Because the method used here cannot treat cases involving sharp edges, the consequences of this assumption are difficult to estimate. Additional calculations were performed for a 5-μm pore with shorter entrance and exit regions. A 43% reduction in length ($\lambda = 0.35\ \mu m^{-1}$) led to an 18% increase in transit time. These calculations suggest that rounded edges ease red cell passage, decreasing transit time.

Populations of circulating red blood cells show distributions of volumes and surface areas. According to the above results, changes in cell volume have appreciable effects on cell transit times, relative to the effects of substantial changes in membrane mechanical properties. Therefore, any volume changes should be allowed for if filtration data are interpreted in terms of membrane mechanical properties. If volume changes are known, correction for volume changes can be carried out simply, based on the estimates presented earlier.

The internal viscosity of the red blood cell is neglected in the above results. An order-of-magnitude estimate of its effect may be obtained by defining the dimensionless number $\mu_{int}r/\mu_m$ where μ_{int} is the internal viscosity and r is the radius of the cell. With typical values $\mu_{int} = 0.06$ dyn·s/cm^2 and $r = 2.5\ \mu$m, this number is 0.015, suggesting that internal viscosity represents a small part of a normal cell's viscous resistance to deformation. To check this, further calculations of cell motion and deformation were performed including the effects of internal viscosity. At each time step, the components of velocity in the interior of the cell were expressed as polynomials in r and z. The coefficients of these polynomials were chosen to satisfy the governing Stokes equations exactly, and to provide least-squares fits with the membrane velocity. Adequate fits were obtained using fifth-order polynomials. The resulting components of fluid stress on the inside of the membrane were inserted into the equations of membrane equilibrium in the system previously described, giving new estimates of membrane velocity. This procedure was repeated iteratively until convergence was achieved, usually within a few iterations. In all cases considered, inclusion of the effects of normal internal viscosity led to a 2–4% increase in predicted transit time. However, if internal viscosity were increased by more than 10-fold, as can occur in sickle cell disease, its effect might be significant.

Another simplifying assumption in the model is the neglect of membrane bending resistance. Consequently, the shape of the high-curvature region at the trailing edge of the cell is not accurately represented. Nonetheless, Secomb et al. (1986) showed that this approach gives estimates of resistance to cell motion in uniform tubes that agree well with calculations including bending resistance. For cell motion in 6.3-μm pores, we performed additional simulations including bending resistance. Except in the rear part of the cells, the resulting cell shapes agreed closely with those obtained neglecting bending resistance.

Our results (Fig. 5) show that transit time is much more sensitive to membrane viscosity than to membrane elasticity, for a wide range of conditions. This finding may be understood by defining a membrane viscous time scale, $T_v = \mu_m/\kappa = 170$ ms. If the time scale of deformations is less than this, membrane shear viscosity dominates effects of shear elasticity. Thus, transit time can only be expected to be sensitive to membrane elasticity if it is of the order of 170 ms or more. This is also evident from a comparison of Figs. 4 and 5. It follows that relatively low driving pressures and/or narrow pores should be used in order to detect moderate alterations in membrane elastic properties. However, our analysis indicates that greater (more than twofold) increases in membrane shear elasticity should be detectable at higher driving pressures.

The effects of membrane shear elasticity and viscosity on transit time were studied experimentally by Frank and Hochmuth (1988). Membrane shear viscosity was approximately doubled by exposure to wheat germ agglutinin, whereas shear elasticity was doubled by heat treatment. In each case, transit time was increased by these treatments, with the largest increases in the smallest pores, as predicted by the model. Doubling membrane viscosity increased transit times in 3.6-, 5- and 6.3-μm pores by 42%, 35%, and 16%, respectively. These increases are of similar magnitude but smaller than our predicted values of 62%, 47%, and 31% for corresponding pressure drops. Doubling membrane elasticity increased observed transit times for the same pores by 40%, 6%, and 2%, respectively, versus predicted increases of 8%, 2%, and 0%. In this case, the observed increases are substantially larger than predicted, although they show the same trend with pore diameter. Overall, therefore, the model predictions are of the same magnitude as these experimental results and show similar trends, although significant quantitative differences exist. These may result from model simplifications or from the difficulty of controlling membrane properties precisely in the experiments.

Drochon et al. (1993) measured filtration rates of normal and diamide-treated red cells through filters with pores 4.7 μm in diameter and 11 μm in length. The membrane elasticity of diamide-treated cells was slightly more than double that of normal cells. When a standard buffer was used as the suspending medium, the filtration rate of diamide-treated cells was the same as that of normal cells, but when suspending medium viscosity was elevated eightfold,

treated cells filtered significantly more slowly than normal cells. On the basis of these observations, Drochon et al. (1993) proposed that changes in red cell membrane properties may be detected more readily by using a suspending medium with high viscosity.

Our results (Fig. 6) imply that the sensitivity to membrane shear elasticity is not strongly dependent on suspending medium viscosity, whereas sensitivity to membrane viscosity decreases with increasing medium viscosity. Therefore, our results do not suggest any particular advantage in the use of higher suspending medium viscosities to detect alterations in membrane mechanical properties. However, the inconsistency between our results and those of Drochon et al. (1993) remains to be resolved.

Recently, Pries et al. (1994) showed that resistance to blood flow in microvessels in vivo is substantially higher than in uniform glass tubes of corresponding diameters. One possible cause for this difference is that microvessels are nonuniform, and red cells must undergo continual transient deformations in traversing them. The energy dissipated in these deformations depends strongly on red cell membrane viscosity and may contribute significantly to resistance to blood flow (Secomb and Hsu, 1996). Therefore, our prediction that results of filtration tests are sensitive to membrane viscosity supports the view that such tests provide a measure of blood's ability to flow through the microcirculation of living tissues.

CONCLUSIONS

We have developed a theoretical model for the motion of red cells through micropores, including effects of viscous and elastic resistance of membrane to shear deformation. Predicted cell transit times are consistent with experimental measurements. Time taken to enter the pore represents at least one-half of the transit time. According to the model, transit time is sensitive to membrane shear viscosity, but insensitive to internal cytoplasmic viscosity for normal cells. At driving pressures typically used in filtration experiments, changes in membrane shear elasticity have little effect on transit time, although their effect increases at very low driving pressures. Changes in cell volume and initial shape can have an appreciable influence on transit time. Increasing suspending medium viscosity does not appear to increase the sensitivity of transit time to membrane properties. We conclude that the filterability of red blood cells is sensitively dependent on their resistance to transient deformations.

Supported by National Institutes of Health grants HL34555 and HL07249.

REFERENCES

Bucherer, C., J. C. Lelièvre, and C. Lacombe. 1988. Theoretical and experimental study of the time dependent flow of red blood cell suspension through narrow pores. *Biorheology.* 25:639–649.

Drochon, A., D. Barthes-Biesel, C. Bucherer, C. Lacombe, and J. C. Lelièvre. 1993. Viscous filtration of red blood cell suspensions. *Biorheology.* 30:1–8.

Drochon, A., D. Barthes-Biesel, and A. Leyrat-Maurin. 1994. Passage of an erythrocyte through a pore: an analysis in terms of cell membrane mechanical properties. *Clinical Hemorheology.* 14:290.

Evans, E. A., and R. M. Hochmuth. 1976. Membrane viscoelasticity. *Biophys. J.* 16:1–11.

Evans, E. A., and R. Skalak. 1980. Mechanics and Thermodynamics of Biomembranes. CRC Press, Boca Raton, Florida.

Fisher, T. C., R. B. Wenby, and H. J. Meiselman. 1992. Pulse shape analysis of RBC micropore flow via new software for the cell transit analyser (CTA). *Biorheology.* 29:185–201.

Fitz-Gerald, J. M. 1969. Mechanics of red-cell motion through very narrow capillaries. *Proc. Roy. Soc. London B.* 174:193–227.

Frank, R. S., and R. M. Hochmuth. 1987. An investigation of particle flow through capillary models with the resistive pulse technique. *J. Biomech. Eng.* 109:103–109.

Frank, R. S., and R. M. Hochmuth. 1988. The influence of red cell mechanical properties on flow through single capillary-sized pores. *J. Biomech. Eng.* 110:156–110.

Gregersen, M. I., C. A. Bryant, W. Hammerle, S. Usami, and S. Chien. 1967. Flow characteristics of human erythrocytes through polycarbonate sieves. *Science.* 157:825–827.

Halpern, D., and T. W. Secomb. 1991. Viscous motion of disc-shaped particles through parallel-sided channels with near minimal widths. *J. Fluid Mech.* 231:545–560.

Hsu, R., and T. W. Secomb. 1989. Motion of non-axisymmetric red blood cells in cylindrical capillaries. *J. Biomech. Eng.* 111:147–151.

Kiesewetter, H., U. Dauer, M. Gesch, D. Seiffge, B. Angelkort, and H. Schmid-Schönbein. 1981. A method for the measurement of the red blood cell deformability. *Scand. J. Clin. Invest.* 41:229–232.

Koutsouris, D., M. Hanss, and R. Skalak. 1983. Determination of erythrocytes transit times through a 5 μ "Nuclepore" filter. *Biorheology.* 20:779–787.

Koutsouris, D., R. Guillet, J. C. Lelièvre, M. Boynard, M. T. Guillemin, P. Bertholom, R. B. Wenby, Y. Beuzard, and H. J. Meiselman. 1988. Individual red blood cell transit times during flow through cylindrical micropores. *Clinical Hemorheology.* 8:453–459.

Lipowsky, H. H., L. E. Cram, W. Justice, and M. J. Eppihimer. 1993. Effect of erythrocyte deformability on in vivo red cell transit time and hematocrit and their correlation with in vitro filterability. *Microvasc. Res.* 46:43–64.

Nakamura, T., S. Hasegawa, H. Shio, and N. Uyesaka. 1994. Rheologic and pathologic significance of red cell passage through narrow pores. *Blood Cells.* 20:151–165.

Nash, G. B. 1990. Filterability of blood cells: methods and clinical applications. *Clinical Hemorheology.* 10:353–362.

Pries, A. R., T. W. Secomb, T. Geβner, M. B. Sperandio, J. F. Gross, and P. Gaehtgens. 1994. Resistance to blood flow in microvessels in vivo. *Circ. Res.* 75:904–915.

Reinhart, W. H., and S. Chien. 1985. Roles of cell geometry and cellular viscosity in red cell passage through narrow pores. *Am. J. Physiol.* 248:C473–C479.

Reinhart, W. H., C. Huang, M. Vayo, G. Norwich, S. Chien, and R. Skalak. 1991. Folding of red blood cells in capillaries and narrow pores. *Biorheology.* 28:537–549.

Secomb, T. W. 1991. Red blood cell mechanics and capillary blood rheology. *Cell Biophys.* 18:231–251.

Secomb, T. W., and J. F. Gross. 1983. Flow of red blood cells in narrow capillaries: role of membrane tension. *Int. J. Microcirc. Clin. Exp.* 2:229–240.

Secomb, T. W., and R. Hsu. 1996. Motion of red blood cells in capillaries with variable cross-sections. To appear in *J. Biomech. Eng.*

Secomb, T. W., R. Skalak, N. Özkaya, and J. F. Gross. 1986. Flow of axisymmetric red blood cells in narrow capillaries. *J. Fluid Mech.* 163:405–423.

Skalak, R., and N. Özkaya. 1987. Models of erythrocyte and leukocyte flow in capillaries. *In* Physiological Fluid Dynamics II. L. S. Srinath and M. Singh, editors. Tata McGraw-Hill, New Delhi. 1–10.